

Numerical Studies of the KP Line Solitons

by Michelle Osborne & Tommy McDowell

Abstract

The Kadomtsev-Petviashvili (KP) equation describes the motion of shallow water waves on a flat two-dimensional region. It admits a class of solitary wave solutions, called line-soliton solutions, which are localized along distinct lines in the xy -plane. These types of solutions have been studied extensively in recent years. Using a variety of initial conditions, the KP equation is simulated numerically, and the interactions of the evolved solitary wave patterns are studied. The goal is to determine to which of the many exact solutions of the KP equation the initial conditions converge.

Introduction

An important example of physically interesting nonlinear wave equations was proposed in 1970 by Kadomtsev and Petviashvili [1] in their study of plasma waves. It is a $(2 + 1)$ -dimensional, weakly nonlinear dispersive wave equation of the form:

$$(4u_t + 6uu_x + u_{xxx})_x + 3u_{yy} = 0, \quad (1)$$

where $u = u(x, y, t)$ represents the (normalized) wave amplitude. Equation (1) is referred to as the KP equation. From a physical perspective, the KP equation has been studied in the context of oblique interactions of ion-acoustic and shallow water solitary waves. An example of such wave phenomena observed in nature is the surface wave patterns created by the oblique interaction of incoming waves in shallow water on long, flat beaches as shown in Figure 1.

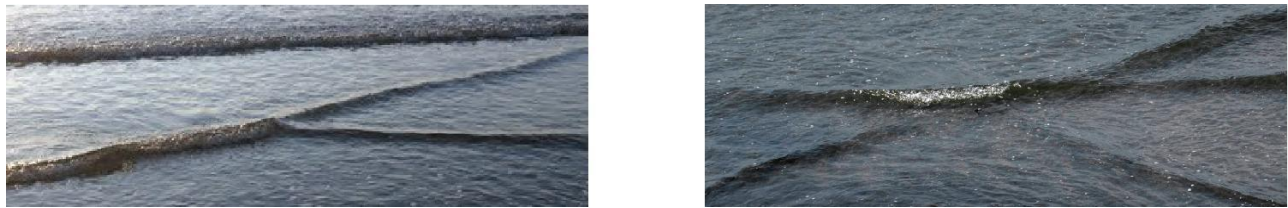


Figure 1: Beach wave patterns. Photographs by M. J. Ablowitz and D. E. Baldwin [2]

The KP equation (1) admits an important class of solitary wave solutions that are regular, non-decaying and localized along distinct lines in the xy -plane. These are known as the line-soliton solutions, which have been studied extensively in recent years [3, 4].

The simplest example of a KP line-soliton is the one-soliton solution, which is a traveling wave:

$$u(x, y, t) = \frac{1}{2}(k_2 - k_1)^2 \operatorname{sech}^2 \frac{1}{2}(k_2 - k_1)[x + (k_1 + k_2)y - ct - x_0], \quad (2)$$

and is localized along a line $L_{12} : x + (k_1 + k_2)y - ct - x_0 = 0$ in the xy -plane for fixed t , as shown in Figure 2. The one-soliton is characterized by two real, distinct parameters $k_1 < k_2$ which determine the *soliton amplitude*: $\frac{1}{2}(k_2 - k_1)^2$, *soliton speed*: $c = k_1^2 + k_1k_2 + k_2^2$, and the *soliton direction* $k_1 + k_2 = \tan(\Psi)$, where Ψ is the angle, measured counterclockwise between the line L and the positive y -axis. We usually denote a one-soliton solution as the [1, 2]-soliton because of its dependence on the parameters k_1, k_2 . The general line-soliton solutions of KP can be constructed in a simple algebraic way as

$$u(x, y, t) = 2(\ln \tau)_{xx}, \tag{3}$$

where the τ -function is a linear combination of exponential functions where the exponents are *linear* in x, y, t .

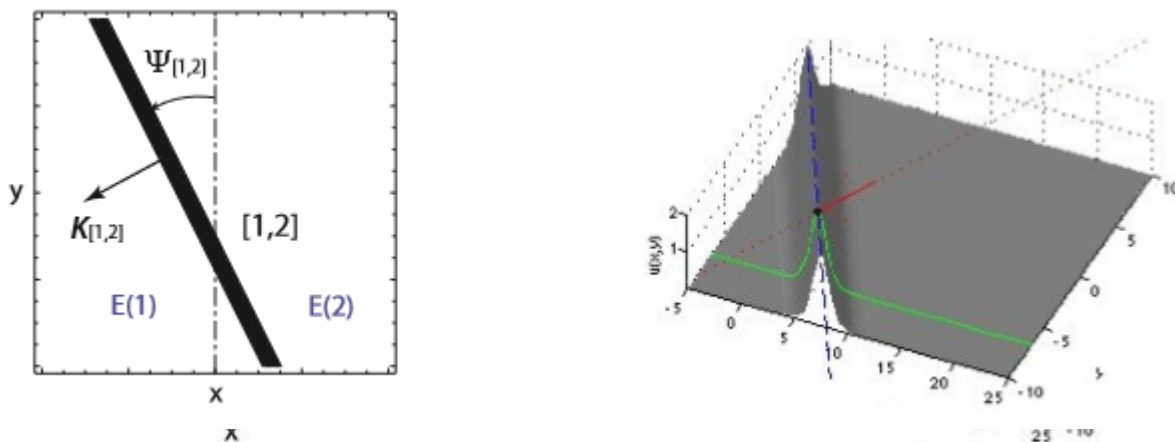


Figure 2. One-soliton solution of KP

Furthermore, the coefficients in the linear combinations are *positive*, which ensures that the solutions obtained via (3) are globally regular. For example the τ -function for the one-soliton solution is given by $\tau(x, y, t) = E(1) + E(2)$ where $E(i) = \exp(k_i x + k_i^2 y + k_i^3 t + \delta_i)$, $i = 1, 2$ where the k_i, δ_i are constants. Note from Figure 2 that the one-soliton solution is exponentially small in regions of the xy -plane where the exponentials $E(1)$ and $E(2)$ are dominant, but is localized along the line L_{12} where $E(1), E(2)$ are of the same order.

In this project, we numerically investigate the interaction properties of the line-soliton solutions corresponding to a variety of initial conditions. We study the convergence of initial data to the exact solutions, and the relation between the parameters defining the initial conditions and those of the exact solution. We consider types of initial waves relevant to physical problems and experiments. Since (1) admits a large number of exact solutions, an important problem is to predict to which exact solution of KP a given initial condition, which resembles a physical interaction of two localized waves, converges. There exist some theoretical conjectures to predict which initial condition would evolve to a given exact solution, but it needs to be supported by the numerical results of this project, which is expected to yield further insight into developing an exact analytical theory.

Numerical Scheme

We are currently developing MATLAB codes to run these numerical simulations, which involve solving the KP equation (1) numerically with given initial data. The efficiency of the codes is being tested using various types of initial data and carefully estimating the error between the exact and numerical solutions of the KP equation. The error is then minimized by optimizing the parameters of the exact solution.

We solve the KP equation numerically using a pseudo-spectral scheme on a rectangular domain $D = \{(x, y) : |x| \leq L_x/2, |y| \leq L_y/2\}$. We assume that the solution is periodic in both x and y .

Then it is convenient to rescale the D to a fixed domain $D' = \{(X, Y) : |X| \leq \pi, |Y| \leq \pi\}$ by defining $X = (2\pi/L_x)x$, $Y = (2\pi/L_y)y$ so that (1) becomes:

$$(u_t + Puu_x + Qu_{3x})_x + Ru_{yy} = 0, \quad P = \frac{3\pi}{L_x}, Q = \frac{2\pi^3}{L_x^3}, R = \frac{6\pi L_x}{4L_y^2}. \quad (4)$$

Due to periodicity, we can express the solution as:

$$u(X, Y, t) = \sum_{l=-\infty}^{\infty} \sum_{m=-\infty}^{\infty} \hat{u}(l, m, t) e^{i(lX+mY)},$$

and reduce (4) into an ODE for the time evolution of the Fourier coefficients $\hat{u}(l, m, t)$, namely,

$$\hat{u}_t + \frac{i l P}{2} N(\hat{u}) + i \left(\frac{R m^2}{l} - Q l^3 \right) \hat{u} = 0, \quad l \neq 0, \quad (5)$$

where $N(\hat{u})$ is the Fourier transform of u^2 which is numerically evaluated as $N(\hat{u}) = FFT \left((IFFT(\hat{u}))^2 \right)$. The ODE (5) can be expressed as:

$$\hat{v}_t + \alpha e^{ct} N(\hat{v} e^{-ct}) = 0,$$

where $c = i(Rm^2/l - Ql^3)$, $\hat{v} = \hat{u} e^{ct}$, $\alpha = ilP/2$, and numerically solved using the Runge-Kutta of order 4 (RK4) method for a given initial data $\hat{u}(l, m, 0)$ obtained from the Fourier Transform of $u(X, Y, 0)$. The solution $u(X, Y, t)$ (hence $u(x, y, t)$) is then reconstructed by taking the inverse Fourier Transform of $\hat{u}(l, m, t)$ for $l \neq 0$.

Remarks

- When $l = 0$, the ODE in (5) reduces to $\hat{u}(0, m, t) = 0$ for all values of m and t . This is called the *zero-mode* condition which is also equivalent to the *mean-free* condition: $\int_{-\pi}^{\pi} u dX = 0$, and must be satisfied for all periodic solutions. Our initial data (in the form of line-solitons) do *not* satisfy the mean-free condition, so we force the zero-modes $\hat{u}(0, m, t)$ to be zero in our numerical code. However, our numerical experiments suggest that the overall error due to the violation of this condition remains small.
- The pseudo-spectral scheme works well for vanishing boundary conditions in both x and y directions. However, the initial data used in our numerical simulations do *not* vanish at the boundaries of the numerical domain D . As a result, in our numerical simulations, the amplitude of the wave near the boundary diminishes, and the crest of the incident solitary wave is bent

backward. To address this issue, we use a method developed by Tanaka [5] (see also [6]) to artificially modify the data near the boundary to maintain constant amplitude and the original shape. For the kind of initial data used in our numerical simulations, we modify the numerical solution by imposing zero boundary conditions in the x -direction, and by “patching” with the exact one-soliton solutions in the y -direction, near the boundary. Figure 3 below shows an example of a V-shape initial condition with the indicated patching region at the boundary.

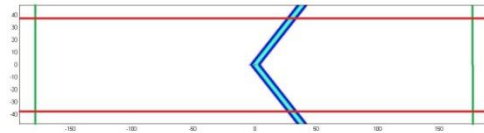


Figure 3. A V-shape initial condition with patching

Simulations and Results

In this section we present numerical simulations which show the evolution of various types of solitary wave initial data to the exact solution of the KP equation. A typical initial condition is formed by gluing together pieces of $[i, j]$ one-soliton solutions of the form:

$$u(x, y, 0) = \frac{1}{2}(k_j - k_i)^2 \operatorname{sech}^2 \frac{1}{2}(k_j - k_i)[x + (k_i + k_j)y - x_0], \quad (6)$$

for different values of the parameters k_i, k_j . In this context, gluing means using half of one soliton and half of another soliton with different k_i and k_j values and joining the two ends together.

Y-soliton

The Y-soliton represents a resonant interaction of 3 one-soliton solutions. In our numerical experiments, we take the initial data consisting of a $[1, 3]$ and $[1, 2]$ soliton glued together as shown in the left frame of Figure 4. The k -parameters are chosen to be $\{k_1, k_2, k_3\} = \{-1, 0, 1\}$. The middle frame ($t = 10.05$) of Figure 4 shows the formation of the $[2, 3]$ soliton as well as dispersive waves created due to the interaction of the initial waves at the intersection point (junction of the Y-shape). The Y-soliton moves faster and eventually separates from the dispersive waves as shown in the right panel ($t = 21$) of Figure 4.

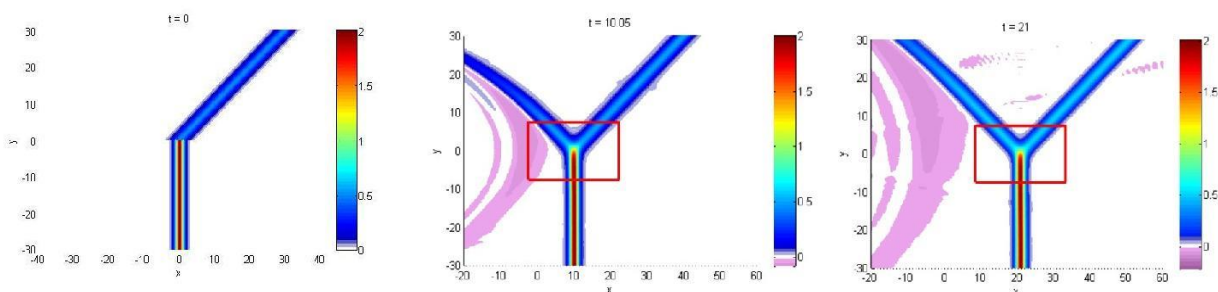


Figure 4: Numerical simulation of a Y-soliton

Next we demonstrate numerically that the initial waves converge to the exact solution. By convergence we mean that the numerical solution in the interaction region generates a pattern due to the

resonant interaction, and this pattern can then be identified with an exact solution of KP. The convergence is only in a local sense; we use the following (relative) error estimate,

$$E(t) = \left[\frac{\iint_B |u_{num}(x, y, t) - u_{exact}(x, y, t)|^2 dx dy}{\iint_B u_{exact}^2(x, y, t) dx dy} \right]^{\frac{1}{2}}, \quad (7)$$

where the L^2 norms are computed over a rectangular box B (shown in Figure 4) around the interaction region. The exact Y-soliton solution is given by (3) where the τ -function is given by

$$\tau = (k_2 - k_1)e^{\theta_1 + \theta_2} + a(k_3 - k_1)e^{\theta_1 + \theta_3} + b(k_3 - k_2)e^{\theta_2 + \theta_3}, \quad a, b > 0, \quad (8)$$

with $\theta_i = (x, y, t) = k_i x + k_i^2 y - k_i^3 t$, $i = 1, 2, 3$. We take the same k -parameters for the numerical and exact solution, and optimize the parameters a, b so that the error in (6) is minimum at a given value of t and decreases for later times. This process identifies an exact solution (with the optimized parameters) that is *closest* to the numerical solution. Figure 5 shows the convergence of the numerical solution to an exact Y-soliton with optimized value of the parameters $\{a, b\} = \{0.605, 1.22\}$

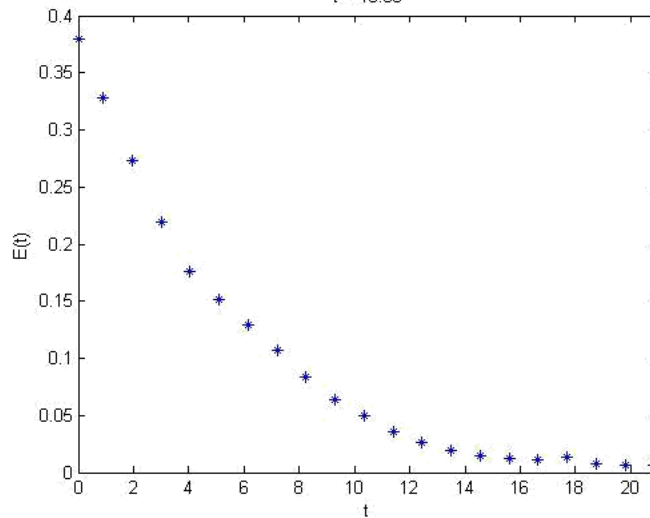


Figure 5. $E(t)$ vs t . Optimized at $t=16$

<- shape initial data

In this example we demonstrate the evolution of a <-shape initial data. The left frame in Figure 6 shows a <-shape initial condition formed by gluing together two one-soliton solutions with k -parameters $\{k_1, k_2, k_3, k_4\} = \{-0.9, -0.1, 0.1, 0.9\}$. The top and bottom solitons of the <-shape are [1, 3] and [2, 4] solitons, respectively. The middle and right frames show the time-evolution of the initial condition at $t = 10$ and $t = 30$, respectively. The initial data converges to a 2-soliton solution of KP called the (3142)-soliton (see e.g. [3]), which consists of [1, 3] and [3, 4] solitons for $y > 0$, [1, 2] and [2, 4] solitons for $y < 0$, and an intermediate [1, 4] soliton in the form of a vertical stem. Note that the dispersive waves created near the intersection point of the <-shape gradually separates from the solitary wave pattern as the (3142) soliton is formed.

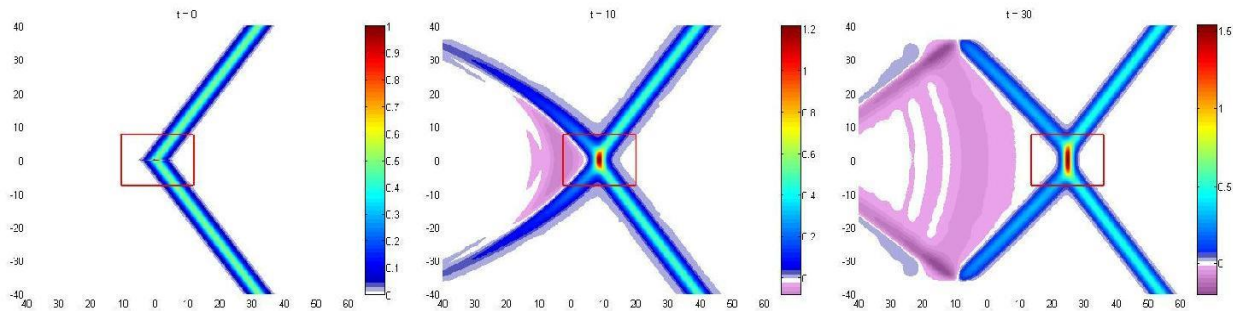


Figure 6. Evolution of a <-shape initial wave

The τ -function for the exact (3142)-soliton depends on k_i and 3 other positive parameters a, b, c . It is given by

$$\sum_{1 \leq i < j \leq 4} A[ij](k_j - k_i)e^{\theta_i + \theta_j}, \tag{8}$$

with $\theta_i = k_i x + k_i^2 y - k_i^3 t$, $i = 1, \dots, 4$, and where $A[12] = 0, A[13] = 1, A[14] = b, A[23] = a, A[34] = c, A[24] = ab$. Like the Y-soliton case, here we choose the same values for the k -parameters which defined the initial <-shape waveform, and optimize the parameters a, b, c so that the error defined by equation (6) is minimized. For this experiment, the optimal parameter values determining the exact (3142)-solution were computed at $t = 20$, and are given by $\{a, b, c\} = \{2.07, 0.23, 0.6\}$. The strictly monotonic decrease of $E(t)$ shown below in Figure 7 indicates that the numerical solution is converging to the exact (3142)-solution.

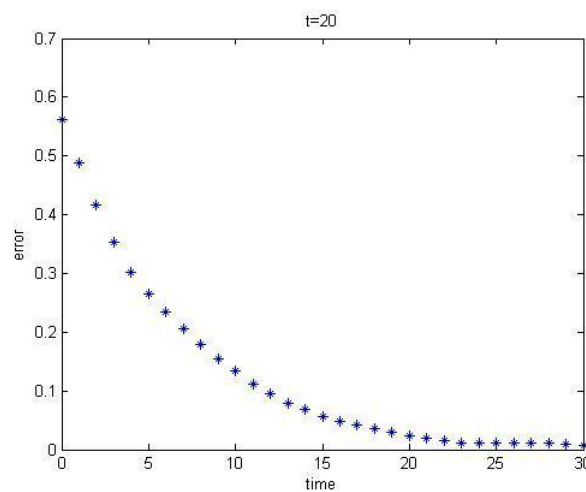


Figure 7. $E(t)$ vs t . Optimized at $t=20$.

Stem of the (3142)-soliton: The stem soliton is formed by the resonant interactions of the [1, 3] and [3, 4] solitons for $y > 0$, and the [1, 2] and [2, 4] solitons for $y < 0$. It is the middle (high intensity) region

shown in the right frame of Figure 6. According to KP theory, the stem is a $[1, 4]$ soliton which depends on the parameters k_1 and k_4 . From (2) the amplitude and velocity of the stem are: $\frac{1}{2}(k_4-k_1)^2$ and $k_1^2 + k_4^2 + k_1k_4$, respectively. We estimate both amplitude and velocity of the stem from the numerical solution and compare them with the theoretical values. The left frame in Figure 8 is a plot of the stem amplitude measured at $y = 0$ with time. As the stem develops, its amplitude grows and gets closer asymptotically (from below) to the theoretical value: $\frac{1}{2}(k_4-k_1)^2 = 1.62$ shown by the solid line in the graph. The growth rate of the amplitude is slow, and the numerically estimated value stays well below the asymptotic value even for much larger run times. The right frame of Figure 8 shows the location of the point on the stem at $y = 0$ as it evolves in time. The graph is linear whose slope yields a numerical estimate of the stem speed. For this simulation, the numerically estimated stem speed = 0.812, which is in agreement with the theoretical value of $k_1^2 + k_1k_4 + k_4^2 = 0.81$.

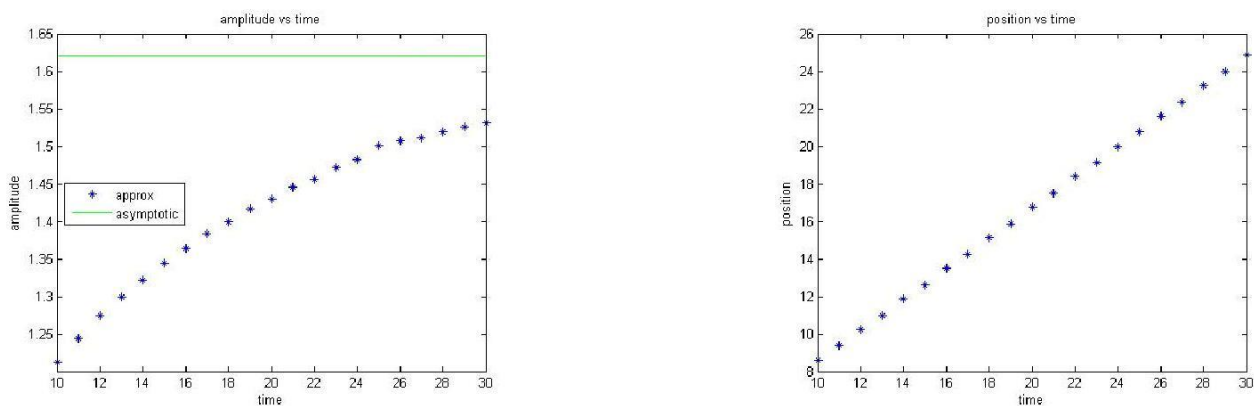


Figure 8. Stem amplitude & position for <-shape initial data

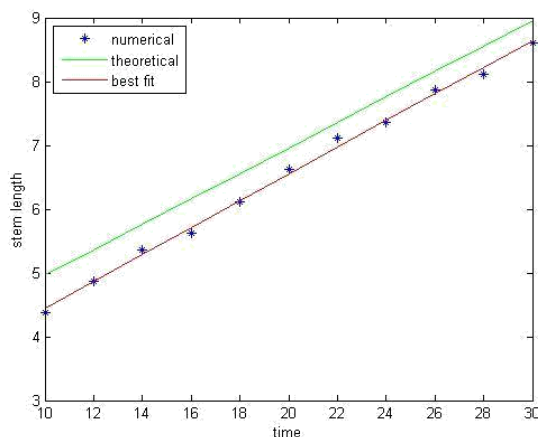


Figure 9. Growth of stem length for <-shape initial data

It should be clear from Figure 6 that the stem evolves to an intermediate soliton whose length increases with time. The theoretical estimate of the stem length is given by $L(t) = 2k_3t + L_0$ where L_0 is a constant that depends on the parameters a, b, c and the k_i . We compare the stem length of the numerical

solution with the theoretical estimate in Figure 9. After adjusting for the soliton width, the theoretical (slope = $2k_3 = 0.2$) is a little higher than the best fit line (slope=0.2) for the numerical data. But both lines have almost the same slope.

Bow-shape initial data

Here we consider an initial condition obtained by adding a small vertical stem to the <-shape as shown in the left frame of Figure 10. We call it the bow-shape initial data. The goal here is to study the evolution of the initial stem in more detail. Given a set of k -parameters $\{k_1, k_2, k_3, k_4\}$, we find that there are two distinct cases corresponding to whether the stem *grows* or *shrinks*. These are described below.

Case 1: Here we choose the bow-shape initial data that is symmetric about the y -axis, and consists of a [1, 2] soliton for $y > 0$, a [3, 4] soliton for $y < 0$ and a [1, 4] soliton as the initial stem. The initial data and its time evolution at $t = 10$ and $t = 31$ are shown in Figure 10 below.

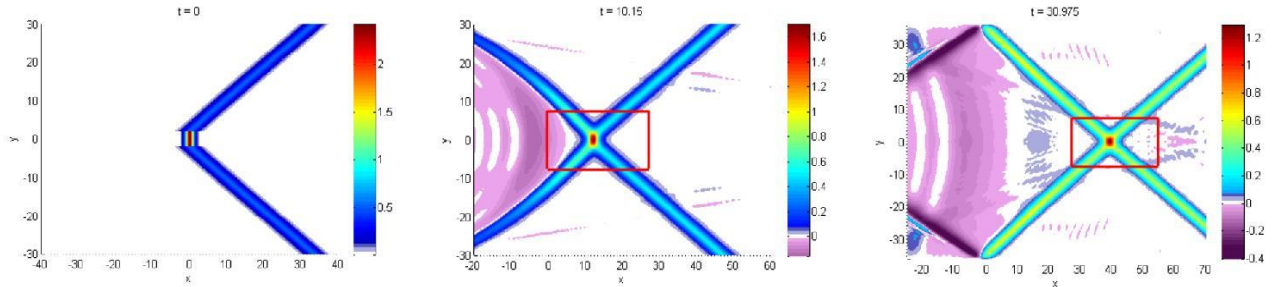


Figure 10. Evolution of a bow-shape initial wave. Initial stem length is 4 units

We observe that the stem in the initial bow shape shrinks with time by shedding energy in the form of dispersive radiation which separates from the solitary waves. The resulting wave pattern from the initial data evolves to an O-type exact solution of KP. The O-type is an X-shape 2-soliton solution with [1, 2] and [3, 4] solitons for both $y > 0$ and $y < 0$ interacting in the middle. We confirm our observation by comparing the numerical solution with an exact O-type solution with optimal parameter values which minimize the error in (6) as discussed earlier. The τ -function for the O-type soliton is given by

$$\tau = (k_3 - k_1)e^{\theta_1 + \theta_3} + a(k_3 - k_2)e^{\theta_2 + \theta_3} + b(k_4 - k_1)e^{\theta_1 + \theta_4} + ab(k_4 - k_2)e^{\theta_2 + \theta_4}, \quad (9)$$

with $\theta_i(x, y, t) = k_i x + k_i^2 y - k_i^3 t$, $i = 1, \dots, 4$. We take the k -parameters to be $\{k_1, k_2, k_3, k_4\} = \{-1.1, -0.1, 0.1, 1.1\}$ for this simulation, the optimal values of the parameters for the exact solution are $\{a, b\} = \{18.3, 1.66\}$. The error plot on the top left frame of Figure 11 shows convergence of this bow-shape initial data to the exact O-type soliton. The top right frame in Figure 11 shows the evolution of the peak amplitude at the interaction region (of the X-shape) for the O-type soliton. As the stem shrinks, the peak amplitude decreases and converges to the theoretically predicted value for the exact O-type soliton. The bottom panel of Figure 11 shows an exact O-type soliton highlighting the maximum of the interaction peak.

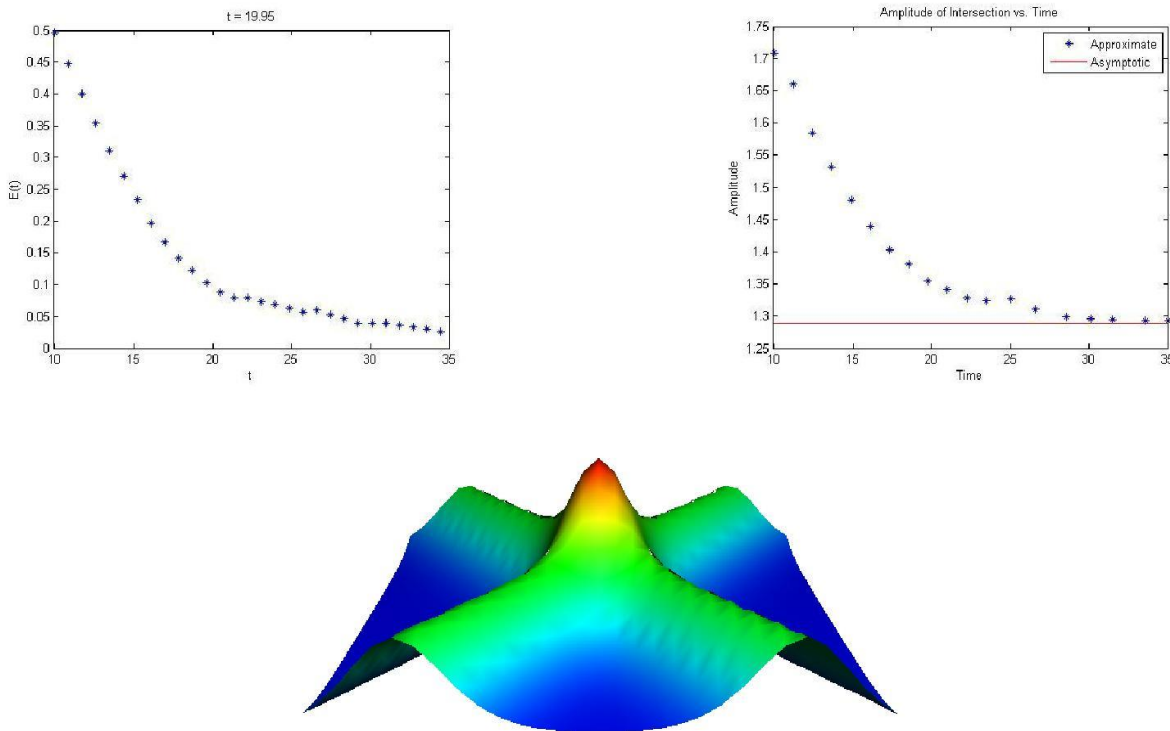


Figure 11. Convergence of a bow-shape initial data to a O-type soliton

The theoretical estimate of the peak amplitude for the O-type soliton was derived in [3], and is given by,

$$u_{max} = A_1 + A_2 + 2\sqrt{A_1 A_2} \left(\frac{1 - \sqrt{\Delta}}{1 + \sqrt{\Delta}} \right), \quad \Delta = \frac{(k_3 - k_2)(k_4 - k_1)}{(k_4 - k_2)(k_3 - k_1)}, \quad (10)$$

where $A_1 = \frac{1}{2}(k_2 - k_1)^2$, $A_2 = \frac{1}{2}(k_4 - k_3)^2$ are the amplitudes of the [1, 2] and [3, 4] solitons, respectively. Using our k -values we obtain $u_{max} = 1.288$ which is what our numerically estimated value approaches to with t .

Case 2: Next we consider a bow-shape initial data which consists of a [1, 3] soliton for $y > 0$, a [3, 4] soliton for $y < 0$ and a [1, 4] soliton as the initial stem with the same set $\{k_1, k_2, k_3, k_4\} = \{-1.1, -0.1, 0.1, 1.1\}$ as in Case 1. The difference between this bow-shape initial data and that of Case 1 is that the amplitudes of the solitons in $y > 0$ and $y < 0$ are higher in this case. The initial data and its time evolution at $t = 10$ and $t = 35$ are shown above in Figure 12. In this case, the stem of the bow-shape grows, and the initial wave form converges to a (3142)-soliton after separating from the dispersive waves. The error between the numerical and the optimal exact (3142)-solution (see previous subsection) with parameters $\{a, b, c\} = \{2.21, 1.38, 0.2\}$ is plotted in Figure 13 below. The error decreases significantly with time, showing convergence to the (3142)-soliton solution, although the error curve is not strictly monotonic as in the previous cases. This is primarily due to the fact that the stem sheds dispersive waves as it grows.

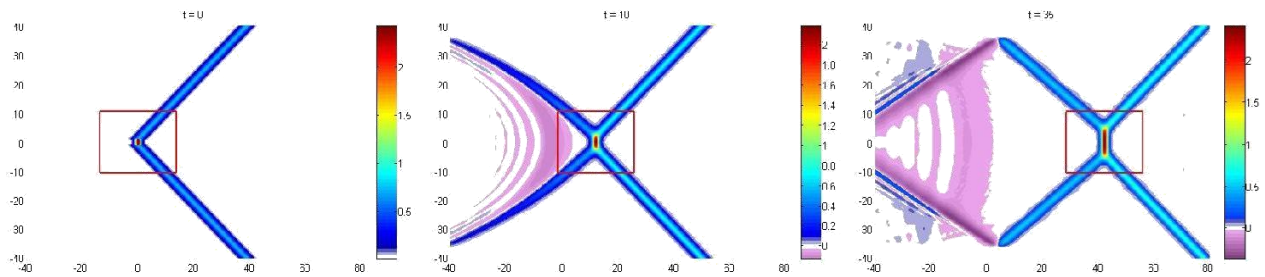


Figure 12. Evolution of a bow-shape initial wave. Initial stem length is 4 units

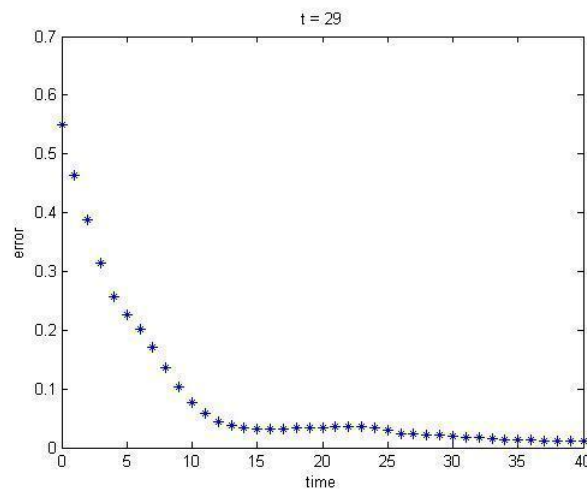


Figure 13. Left: $E(t)$ vs t . Optimized at $t = 29$

Behavior of the stem: In our simulations, we observe that as the stem grows, its shape and amplitude fluctuates considerably due to interaction with dispersive waves. This behavior contrasts the smooth evolution of the stem for the (3142)-soliton corresponding to the \leftarrow -shape initial data discussed earlier. Hence, instead of computing the stem amplitude only at $y = 0$ (as in the previous case), here we compute the average amplitude over a region around the center ($y = 0$) of the stem, and compare with the theoretical value. Figure 14 shows our results. The left frame is a plot of the average stem amplitude with time, and shows that the stem amplitude grows asymptotically, and gets much closer to the theoretical value than in the case of the \leftarrow -shape initial data (cf. Figure 8). The average stem amplitude at $t = 40$ is 2.4 while the theoretical value is 2.42. The middle frame shows the evolution of the center of the stem at $y = 0$. The slope of this curve matches almost exactly with the theoretical value of the stem velocity $k_1^2 + k_1k_4 + k_4^2 = 1.21$. The right panel shows the plot of the numerically estimated stem length versus time. This growth is almost linear as predicted by KP theory; the slope of the theoretical line is $2k_3 = 0.2$, while the slope of the best fit line through the numerical data is 0.205. However, the numerically estimated values for the actual stem length seem to be larger than the theoretical values for all t . We believe that this discrepancy (see also Figure 9) is mainly due to the method used to numerically estimate the stem length. We are trying to improve our current method.

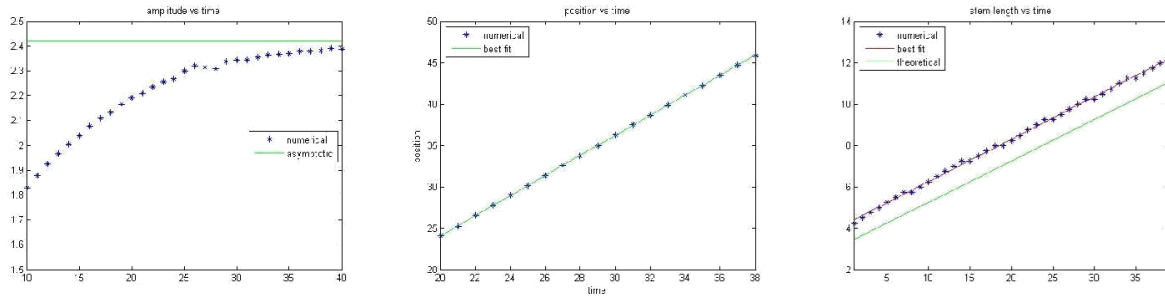


Figure 14. Stem growth for a bow-shape initial data

Conclusion

In our simulations, we numerically investigated the initial value problem of the KP equation. In the case of the Y-junction, we saw that the initial condition converged to the exact Y-junction solution of KP. In the error plot, the error is high at first since our initial condition is not an exact solution. As time progresses, the error decreases indicating that the initial condition is in fact converging to the Y-junction solution. We also studied the <-shape initial condition. The stem forms and continues to grow over time. This behavior is typical for the (3142) case. Two bow-shape initial conditions have also been investigated. In one case, the stem increases and converges to (3142). In the other case, the stem decreases to a point and converges to the O-type solution. To be sure of the convergence of a particular initial condition, further analysis was done. For the (3142) bow-shape initial condition, we looked at the stem growth rate of the numerical simulation and compared it to the growth rate of the exact solution. The rates nearly matched which provides more confidence in the convergence of the (3142)-solution. Likewise, for the O-type solution, the peak amplitude obtained from the numerical data converged to the theoretical value for the exact O-type solution. Our study confirmed for the evaluated cases that the initial condition converged to a soliton solution of the KP equation.

References

1. B B Kadomtsev and V I Petviashvili, On the stability of solitary waves in weakly dispersing media, *Sov. Phys. Doklady* **15**, 539–541 (1970)
2. M. J. Ablowitz and D. E. Baldwin, Nonlinear shallow ocean-wave soliton interactions on flat beaches, *Phys. Rev. E* **86** (2012) 036305
3. S. Chakravarty and Y. Kodama, Soliton solutions of the KP equation and application to shallow water waves, *Stud. Appl. Math.*, **123** (2009) 83-151.
4. C-Y Kao and Y. Kodama, Numerical study of the KP equation for non-periodic waves, *Math. Comput. Simul.* **82** (2012) 1185–1218.
5. M. Tanaka. Mach reflection of a large-amplitude solitary waves, *J. Fluid Mech.*, **248** (1993) 637661.
6. Y. Jia, *Numerical study of the KP solitons and higher order Miles theory of the Mach reflection in shallow water*, PhD. Thesis, Ohio State University (2014).